

Synthesis and Properties of 5-(3-Pyridyl)porphyrinatoruthenium(II) Tetramers

Kenji Funatsu,[1] Naomi Yasuda,[1] Akio Ichimura,[2] Ryoko Santo,[2] Yoichi Sasaki,[1] and Taira Imamura*[1]

[1]Division of Chemistry, Graduate School of Science, Hokkaido University, Sapporo 060-0810

[2]Department of Chemistry, Faculty of Science, Osaka City University, Osaka 558-0022

Received December 27, 2006; E-mail: timamura@sci.hokudai.ac.jp

5-(3-Pyridyl)porphyrinatoruthenium(II) tetramers, [{Ru(3-PyT$_3$porph)(CO)}$_4$] (**1**), [{Ru(3-PytB$_3$porph)(CO)}$_4$] (**2**), [{Ru(3-PyHex$_3$porph)(CO)}$_4$] (**3**), and [{Ru(3-PytB$_3$porph)(py)}$_4$] (**4**) were prepared. The structures of the isolated tetramers were determined to be rhombic shaped with two chemically nonequivalent porphyrinatoruthenium(II) subunits by ^{1}H NMR, IR, and ESI-MS measurements. The tetramers were stable in benzene at 70 °C. However, the tetramers reacted with a large excess of pyridine to give two geometrical isomers of porphyrinatoruthenium(II) in dichloromethane at room temperature as observed by ^{1}H NMR spectrometry. UV–vis spectra of the tetramers showed splitting or broadening of the Soret band due to excitonic interactions. Stepwise oxidations of the porphyrin rings or the ruthenium ions in the cyclic tetramer skeleton were observed in cyclic voltammograms.

Studies of metalloporphyrin oligomers have been used to gain useful information on various systems. For example, they have been used as model systems for photo-induced electron transfer in photosynthetic reaction centers,[1] as enzymatic catalysts,[2,3] and as models for the intramolecular interactions in the metalloporphyrin subunits.[3–7] In order to gain even more information, new metalloporphyrin oligomers having unique structures and characters must be prepared. The approaches to construct those oligomers include non-covalent ligation and self-assembly of metallo- or free-base-porphyrins with oxo-, pyridyl-, or imidazolyl-substituents.[4–13]

Above all, arylporphyrins with pyridyl groups are very useful for coordinative substituent-directed assembly of multiporphyrins by varying the pyridyl substituents from 2-pyridyl groups to 4-pyridyl groups, because of the relative linear direction of metal–pyridyl bonds. Indeed, metal (Zn,[13] Mg,[14] Ru,[15,16] and Rh[17]) 2-pyridylporphyrins as well as imidazole-tethered porphyrinatozincs[5] have been assembled to give unique slipped-cofacial porphyrin dimers, which have strong intramolecular interactions. On the other hand, in 5-(4-pyridyl)porphyrins, square tetramers for Zn,[18] Ru,[19] and Rh[17] have been prepared. For a 5-(3-pyridyl)porphyrinatozinc with hydroxyphenyl groups[20] and 5-(3-pyridyl)porphyrinatozincs,[21] tetrameric structures with a rhombic shape have been reported. A porphyrinatozinc with a 2-aminopyrimidine moiety, which is similar to the 3-pyridyl group in the position of N-atoms, also forms a tetramer complex.[22] The latter two complexes show a large change in UV–vis spectra at variable temperatures due to dissociation/association equilibria. This behavior results from the breakage of the coordination bonds between zinc ions and nitrogen atoms of pyridyl[21] or aminopyrimidine groups,[22] as generally observed by UV–vis absorption dilution studies on pyridylporphyrinatozinc oligomers.[23] These results motivated us to study metal 3-pyridylporphyrins with robust metal–pyridyl bonds without dissociation/association equilibria.

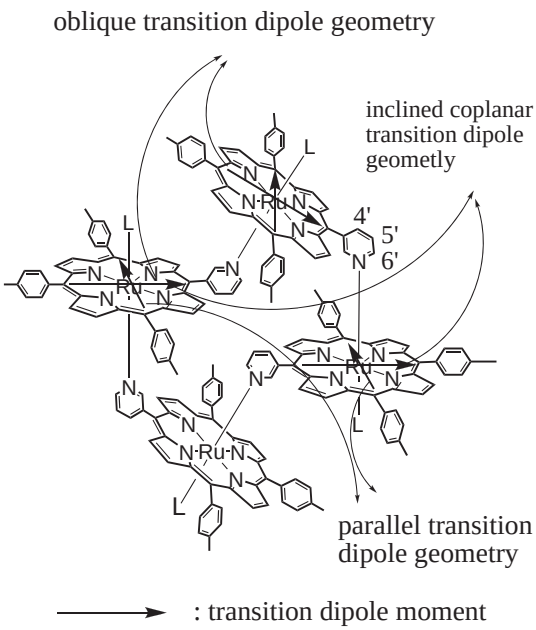

Fig. 1. Proposed structure and excitonic interactions in cyclic tetramers with a rhombic shape. L denotes axial ligands such as CO and pyridine.

In the present work, new 5-(3-pyridyl)porphyrinatoruthenium(II) tetramers were prepared and characterized. ^{1}H NMR measurements proved that these tetramers had a rhombic structure as shown in Fig. 1. UV–vis and electrochemical data showed that there were strong intramolecular interactions between the constituent porphyrin subunits.

Experimental

Instrumentation. UV–vis spectra were recorded on a Hitachi

Published on the web August 10, 2007; doi:10.1246/bcsj.80.1556

U-3000 spectrophotometer. ^{1}H NMR spectra were recorded on a JEOL-EX270 spectrometer. ESI-MS spectral measurements were carried out at Center for Instrumental Analysis, Hokkaido University and GC-MS and NMR Laboratory, Faculty of Agriculture, Hokkaido University using a JEOL JMS-700TZ and a JEOL JMS-SX102 combined with a JEOL MS-ESI 10L2, respectively. Cyclic voltammograms (CVs) were recorded with a BAS model CV-50W voltammetry analyzer with a scan rate of 100 mV s^{-1} at 20 °C. The reference electrodes were an aqueous Ag/AgCl or an Ag/Ag^+ (CH_3CN). The working and the counter electrodes for the CV measurements were a platinum disk (i.d. = 1.6 mm) and a platinum wire, respectively. The sample solutions in dichloromethane containing 0.1 M $Bu_4N(PF_6)$ were deoxygenated by a stream of argon. Redox potentials obtained were referenced to the redox potential of a ferrocenium/ferrocene couple $E^{o\prime}(Fc^+/Fc)$. A digital simulation of CVs was made with the simulation package DigiSim 3.0 (Bioanalytical Systems).

Porphyrin Ligands. 5-(3-Pyridyl)-10,15,20-tri-*p*-tolylporphyrin (H_2(3-PyT$_3$porph)), 5-(3-pyridyl)-10,15,20-tris(*p*-*t*-butylphenyl)porphyrin (H_2(3-PytB$_3$porph)), and 5-(3-pyridyl)-10,15,20-tris(*p*-hexyloxyphenyl)porphyrin (H_2(3-PyHex$_3$porph)),[24] were synthesized by combining 3-pyridinecarbaldehyde and *p*-tolualdehyde, 3-pyridinecarbaldehyde and 4-*tert*-butylbenzaldehyde, and 3-pyridinecarbaldehyde and 4-(hexyloxy)benzaldehyde, respectively, with reference to the literature,[6] and characterized by spectral methods and elemental analyses.

A typical preparation method for H_2(3-PyHex$_3$porph) is as follows. A propionic acid (200 mL) solution containing 4-(hexyloxy)-benzaldehyde (12.5 mL, 60 mmol), 3-pyridinecarbaldehyde (19 mL, 20 mmol), and pyrrole (5.6 mL, 80 mmol) was refluxed for 3.5 h and cooled to room temperature. The solution was filtered off. The resulting solid was dried at 100 °C in vacuo (yield: 1.9 g). The solid (0.9 g) was dissolved in a small amount of dichloromethane and column-chromatographed on silica gel. After the first band of H_2(Hex$_4$porph) was eluted with neat dichloromethane (yield: 750 mg), the second band containing the desired ligand was eluted with 1% MeOH–CH_2Cl_2. The solvent was evaporated, and the residue was dried at 100 °C in vacuo (yield: 170 mg).

Anal. Calcd for $C_{61}H_{65}N_5O_3$ (H_2(3-PyHex$_3$porph)): C, 79.97; H, 7.15; N, 7.64%. Found: C, 79.65; H, 7.16; N, 7.36%. UV–vis λ_{max} (ε 10^4 M^{-1} cm^{-1} in CH_2Cl_2): 421 (49.0), 518 (1.72), 555 (1.12), 593 (0.54), 650 (0.63). ^{1}H NMR ($CDCl_3$, 270 MHz, 23 °C): δ −2.77 (2H, s, NH), 0.98 (9H, t, $OCH_2CH_2(CH_2)_3CH_3$), 1.44–1.66 (18H, m, $OCH_2CH_2(CH_2)_3CH_3$), 1.99 (6H, quin, $OCH_2CH_2(CH_2)_3CH_3$), 4.23 (6H, t, $OCH_2CH_2(CH_2)_3CH_3$), 7.30 (6H, d, *m*-Ph), 7.73 (1H, m, 5-Py), 8.11 (6H, d, *o*-Ph), 8.51 (1H, m, 4-Py), 8.75–8.93 (8H, m, β), 9.03 (1H, m, 6-Py), 9.45 (1H, m, 2-Py). FAB-MS: 916 m/z^+ (M^+).

[{Ru(3-PyT$_3$porph)(CO)}$_4$] (1). Diethylene glycol monomethylether suspension (100 mL) containing H_2(3-PyT$_3$porph) (50 mg, 81 μmol) and $Ru_3(CO)_{12}$ (150 mg, 240 μmol) was refluxed for 2 h under N_2 atmosphere. The reaction was monitored by visible spectroscopy and then heating was stopped when the characteristic band of H_2(3-PyT$_3$porph) at around 650 nm was no longer evident. After standing at room temperature, the solution was passed through sintered glass. To the solution was added a saturated NaCl aqueous solution (100 mL). The resulting precipitate was filtered through sintered glass, washed with water, and dried at 100 °C in vacuo for 1 h. Since the crude product showed a UV–visible band of chlorin at around 600 nm, DDQ was added to a dichloromethane solution of **1**. The suspension was stirred at room temperature until the characteristic band disappeared. DDQ residue was filtered off, and the filtrate was chromatographed on a silica-gel column using dichloromethane as an eluent. The first band was collected and evaporated to dryness. The product was dried at 80 °C in vacuo for 1 h (yield: 12 mg, 19%).

Anal. Calcd for $C_{188}H_{132}N_{20}O_4Ru_4$: C, 71.92; H, 4.24; N, 8.92%. Found: C, 72.22; H, 4.59; N, 8.69%. UV–vis λ_{max} (ε 10^4 M^{-1} cm^{-1}/ε per subunit in CH_2Cl_2): 404 (59.2/14.8), 418 (sh. 51.8/13.0), 535 (7.26/1.82), 570 (2.30/0.58).

[{Ru(3-PytB$_3$porph)(CO)}$_4$] (2). Complex **2** was synthesized by a method similar to that of **1** using H_2(3-PytB$_3$porph) in place of H_2(3-PyT$_3$porph). $Ru_3(CO)_{12}$ (150 mg, 235 μmol) and H_2(3-PytB$_3$porph) (100 mg, 128 μmol) were reacted (yield: 35 mg, 30%).

Anal. Calcd for $C_{224}H_{204}N_{20}O_4Ru_4$: C, 73.82; H, 5.64; N, 7.69%. Found: C, 74.01; H, 5.93; N, 7.82%. UV–vis λ_{max} (ε 10^4 M^{-1} cm^{-1}/ε per subunit in CH_2Cl_2): 407 (65.0/16.3), 415 (sh. 58.7/14.7), 537 (7.63/1.91), 572 (2.45/0.61). ESI-MS: 3644 m/z^+ (M^+).

[{Ru(3-PyHex$_3$porph)(CO)}$_4$] (3). 2-(2-Methoxyethoxy)-ethanol (300 mL) was heated to 80 °C under Ar, and H_2(3-PyHex$_3$porph) (150 mg, 164 μmol) was added. After complete dissolution, $Ru_3(CO)_{12}$ (300 mg, 470 μmol) was added, and the temperature was increased to 150 °C. When no UV–vis spectral changes were observed after 1.5 h, the solution was cooled to room temperature and salted out with an aqueous solution of sodium chloride. After filtering and thoroughly washing with water, the resulting solid material was dried over P_2O_5 under reduced pressure for 12 h and then dissolved in dichloromethane. To the solution, DDQ was added and stirred until no UV–vis peaks of ruthenium–chlorin complexes were observed, and the solution was subjected to chromatography with silica gel. The first red-band that eluted with dichloromethane was collected, and the solvent was evaporated to dryness. The resulting solid was recrystallized from dichloromethane–hexane and dried for 2.5 h under reduced pressure (yield: 25 mg).

Anal. Calcd for $C_{248}H_{252}N_{20}O_{16}Ru_4$: C, 71.38; H, 6.09; N, 6.71%. Found: C, 71.05; H, 6.11; N, 6.79%. UV–vis λ_{max} (ε 10^4 M^{-1} cm^{-1}/ε per subunit in CH_2Cl_2): 407 (64.0/16.0), 419 (sh. 56.5/14.1), 537 (7.38/1.85), 574 (2.82/0.71). IR (KBr mull): ν_{CO} 1951 cm^{-1}, ESI-MS: 4173 m/z^+ (M^+).

[{Ru(3-PytB$_3$porph)(py)}$_4$] (4). A toluene solution (700 mL) containing **2** (25 mg, 6.9 μmol) and pyridine (2.2 μL, 27 μmol) was irradiated with visible light using a medium-pressure mercury lamp for 4 h under vigorous Ar bubbling and stirring at temperatures from 0 to 5 °C. Upon irradiation, the solution color changed from red to brown. The brown solution was filtered and evaporated to dryness. The resulting solid was dissolved in a small amount of toluene and separated by an alumina column (Activity III) with toluene as an eluent. The first eluted brown-band was collected, and the solvent was evaporated to dryness. The resulting deep-purple solid was recrystallized from toluene–methanol and dried at 110 °C in vacuo for 3 h (yield: 23 mg, 85%).

Anal. Calcd for $C_{240}H_{224}N_{24}Ru_4$: C, 74.89; H, 5.87; N, 8.74%. Found: C, 74.85; H, 6.35; N, 8.52%. UV–vis λ_{max} (ε 10^4 M^{-1} cm^{-1}/ε per subunit in CH_2Cl_2): 411 (42.6/10.7), 424 (sh. 41.5/10.4), 510 (7.61/1.90), 534 (sh. 2.70/0.68), 582 (0.89/0.22), 658 (0.38/0.10). ESI-MS: 3849 m/z^+ (M^+).

Results and Discussion

Characterization of Porphyrin Tetramers 1–4. These complexes could not be obtained as single crystals suitable for X-ray crystallography. However, complexes **2–4** were

Table 1. ^{1}H NMR Chemical Shift Values of 3-Pyridylporphyrinatoruthenium(II) Tetramers[a)]

Complex	3-Pyridyl	β-Pyrrole	Phenyl (*o*, *m*)	*tert*-Bu or Hexyloxy	Pyridine (axial ligand)
2 (at 70 °C)	2-Py: 2.31 (s, 2H), 2′-Py: 2.75 (s, 2H) 4-Py: 5.72 (d, 2H), 4′-Py: 6.18 (d, 2H) 5-Py: 3.97 (t, 2H), 5′-Py: 4.70 (t, 2H) 6-Py: 1.07 (d, 2H), 6′-Py: 2.14 (d, 2H)	7–9[b)]	7–9[b)]	0.98 (s, 18H) 1.44 (s, 36H) 1.58 (s, 36H) 1.62 (s, 18H)	
3 (at 23 °C)	2-Py: 2.38 (s, 2H), 2′-Py: 2.91 (s, 2H) 4-Py and 4′-Py: 5.92 (m, 4H) 5-Py: 4.31 (t, 2H), 5′-Py: 4.50 (t, 2H) 6-Py: 1.13 (d, 2H), 6′-Py: 2.08 (d, 2H)	7–9[b)]	7–9[b)]	0.79–1.95 (m, 132H) 3.16 (t, 4H) 3.63–4.05 (m, 20H)	
4 (at 70 °C)	2-Py: 3.34 (s, 2H), 2′-Py: 3.82 (s, 2H) 4-Py: 5.58 (d, 2H), 4′-Py: 6.32 (d, 2H) 5-Py: 4.05 (t, 2H), 5′-Py: 4.72 (t, 2H) 6-Py: 1.98 (d, 2H), 6′-Py: 3.13 (d, 2H)	8.24 8.31 8.37 8.44 8.74 8.90	7–9[b)]	0.98 (s, 18H) 1.45 (s, 36H) 1.50 (s, 36H) 1.63 (s, 18H)	α-Py: 2.75 (d, 4H) β-Py: 4.88 (t, 4H) γ-Py: 5.44 (t, 2H) α-Py′: 2.39 (d, 4H) β-Py′: 4.21 (t, 4H) γ-Py′: 4.88 (t, 2H)

a) In C_6D_6. Chemical shift values in δ were corrected with respect to C_6H_6 (7.2 ppm). b) These proton signals were not precisely analyzed due to broadening.

characterized to be tetramers with a rhombic structure by ^{1}H NMR spectroscopy, IR spectroscopy, electrospray ionization mass spectrometry (ESI-MS), and elemental analysis, as described later in detail. In **1**, its significantly low solubility in organic solvents, such as dichloromethane, chloroform, toluene, and benzene, inhibited the measurements of ^{1}H NMR spectrum for structural analysis. However, mass spectrometry and elemental analysis, and the similarities in UV–vis and IR spectra, and the CVs to those of **2** and **3** supported the formation of the self-assembled porphyrinatoruthenium tetramer with a rhombic shape. The solubility of **2** was much higher than that of **1**, because of the *tert*-butyl substituents. However, contrary to our expectation, the solubility of **2** was lower than the monomeric complex [Ru(tpp)(CO)(py)]. Complex **4** was also less soluble in the solvents, compared to the corresponding monomer analogue of [Ru(tpp)(py)$_2$]. Complex **3** was the most soluble and made it possible to obtain a ^{1}H NMR spectrum at room temperature, while other complex systems were measured at 70 °C (vide infra).

Elemental analyses of all the tetramers agreed well with their respective compositions. Infrared spectra of **1**, **2**, and **3** had characteristic carbonyl-stretches at 1956, 1958, and 1951 cm^{-1}, respectively. Complex **4** showed no carbonyl stretches, indicating thorough decarbonylation from the axial site.

Mass spectroscopy supported the formation of the porphyrin tetramers. ESI-MS of **2**, **3**, and **4** showed respective characteristic peaks corresponding to the molecular weights at 3644.2, 4173.1, and 3848.5 when a mixed solvent of methanol/dichloromethane (4/1 (v/v) for **2** and **4**, and 1/1 for **3**) was used. Under these conditions, **1** showed no clear ESI-MS spectra, because of insolubility in the mixed solvent. However, when dichloromethane was used in the ESI-MS measurements, these porphyrin oligomers appeared as tetramers. The ESI-MS spectrum of **4** showed an intense peak centered at 1924.4412 (100%) with an m/z peak spacing of 0.5 amu (atomic mass unit), corresponding to the 2+ charge state ($[M]^{2+}$). The peak corresponding to 3+ charge state ($[M]^{3+}$) with an m/z peak spacing of 0.33 amu was also obtained at 1282.5948 (7.40%). Calculated molecular weights from the peaks of $[M]^{2+}$ and $[M]^{3+}$ were 3848.3668 and 3847.7844 amu, respectively. These values are in excellent agreement with the theoretical average mass of the porphyrinatoruthenium tetramer of **4** (3848.8823; error = 2.6 ppm for $[M]^{2+}$ and 2.9 ppm $[M]^{3+}$). In the porphyrin oligomers of **1** and **2**, the peaks corresponding to 1+ charge states of porphyrin tetramers were observed at 3139.5850 (13.73%) and 3644.2190 (8.01%), accompanied by intense peaks at 1569.6252 (m/z, 100%) and 1821.8378 (100%), respectively. These latter peaks were ascribed to 2+ charge states of porphyrin tetramers, judging from the sharpness of the intense peaks and ESI-MS features of **4**.

Table 1 listed ^{1}H NMR data of **2**, **3**, and **4**. The spectra of **2** and **4** were measured at 70 °C due to lower solubility in C_6D_6, while the measurement on **3** with hexyloxy groups was carried out at room temperature (23 °C) as described above. At temperatures lower than 90 °C, no rotation of the bridging pyridyl groups and axial pyridyl ligands took place.[19,25] Although β-pyrrole protons gave no clear results, because of broadening of the signals at around 7–9 ppm, up-field shifts of pyridyl proton signals and signal patterns were diagnostic enough to characterize of the porphyrinatoruthenium tetramers having a rhombic form. The proposed structure, depicted in Fig. 1, suggests that the tetramers are composed of geometrical porphyrin isomers, that is, two porphyrin subunits in four porphyrins have a pyridyl group with a *cis*-direction to the axial ligand of L (Py or CO), and the other two porphyrin subunits have a *trans*-pyridyl group (Fig. 2e). Indeed, as summarized in Table 1, each pyridyl group of **2** and **3** showed two different proton signals with the same intensity in the magnetic region between 1–6 ppm. Namely, in **2**, one set of the 3-pyridyl signals on phase sensitive H–H COSY possessed three signals at 1.07 ppm (doublet, 6-Py), 3.97 ppm (triplet, 5-Py), and 5.72 ppm (doublet, 4-Py), as shown in the solid line of Fig. S1. Another set of 3-pyridyl proton signals (6′-Py, 5′-Py, and 4′-Py) appeared at slightly lower fields than each of the signals with

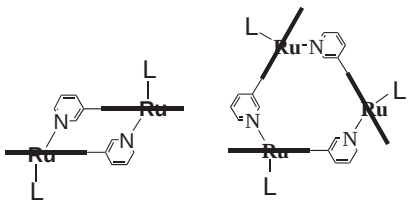

(a) cofacial dimer (b) cyclic trimer

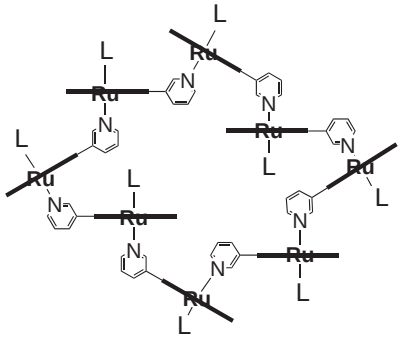

(c) cyclic octamer

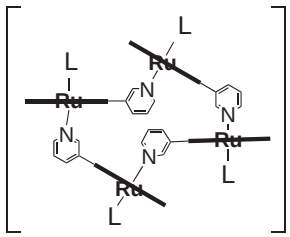

(d) proposed structure with a rhombic shape

cis-subunit *trans*-subunit

(e) porphyrinatoruthenium subunits

Fig. 2. Topologically possible structures of self-assembled 5-(3-pyridyl)porphyrinatoruthenium(II) oligomers (a–d) and their porphyrin subunits (e).

similar correlations. Two additional singlet signals (2H integral intensities) that appeared at 2.31 and 2.75 ppm were assigned to 2-Py protons on 3-pyridyl substituents. These ^{1}H NMR data show that the 3-pyridyl substituents coordinate to ruthenium ions and that two different kinds of porphyrinatoruthenium subunits are present. The NMR results do not support the formation of a slipped cofacial dimers and cyclic trimers illustrated in Figs. 2a and 2b, because these oligomers contain only the same porphyrin subunits with a *trans*-3-pyridyl group, that is, the direction of the each pyridyl N-atom is reverse to that of the CO ligands. Although larger oligomers, such as an octamer, composed of six *cis*-pyridylporphyrins and two *trans*-pyridylporphyrins shown in Fig. 2c, are also topologically possible, the NMR data exclude their formation, because of the difference in the composition ratio of porphyrin subunits.

In the H–H COSY spectrum of **4**, two sets of signals for 3-pyridyl substituents were observed in the region of 2 to 6.5 ppm, as shown in Table 1 and Fig. S2. In addition, axial pyridine exhibited two sets of signals (α-, β-, γ-Py and α-, β-, γ-Py′) in the same region. Although some signals of pyridines were overlapped, correlation of H–H COSY distinguished the two sets of pyridine signals. Thus, no essential differences exist between the NMR data of those tetramers, though the measurement temperatures were different. The ^{1}H NMR and ESI-MS results indicate that the porphyrin oligomers are cyclic porphyrinatoruthenium tetramers with a rhombic shape. This proposed structure is essentially the same with that of 5-(3-pyridyl)porphyrinatozincs, which have been analyzed by using single-crystal X-ray crystallography.[20,21] ^{1}H NMR spectra of monomeric porphyrins formed by dissociation of the tetramers in the presence of a large excess of pyridine also support the rhombic structure composed of two kinds of geometrical isomers (see section of Reaction with Pyridine). This rhombic structure was stable even at 70 °C without dissociation/association. Indeed, no UV–vis spectral changes occurred at different temperatures.

UV–Vis Spectra. UV–vis spectra of **1**, **2**, and **3** exhibited a broad Soret band with an apparent shoulder and two Q bands as shown in Figs. 3a and 3b. In every tetramer, the shape of the Soret band reflected excitonic interactions, stronger than those of square tetramers, [{Ru(4-PyP$_3$porph)(CO)}$_4$] and [{Ru(4-PyT$_3$porph)(CO)}$_4$].[19] Excitonic splittings in the Soret bands of **1**, **2**, and **3** were evaluated from the wavelengths of the peaks and shoulders as 829, 529, and 704 cm^{-1}, respectively. Both the main interactions between inclined coplanar dipole–dipoles and between obliquely arranged dipole–dipoles, illustrated in the Fig. 1, explain the splitting of the Soret band of porphyrins **1**, **2**, and **3**.[26] Q bands of the porphyrin tetramers were red-shifted slightly relative to those of monomers, such as [Ru(tpp)(CO)(py)], as observed in many porphyrinatozinc dimers aligned coplanarly.[27] In the pyridine complex of **4**, the Soret band was also broader than that of the corresponding monomer of [Ru(tB$_4$porph)(py)$_2$] as shown in Fig. 3c, reflecting excitonic interactions. The Q band was shifted 4 nm from 506 nm of the monomer to lower energy (510 nm).

Reactions with Pyridine. By the addition of an excess of pyridine (final concentration ratio: 10^4–10^5 times) to the dichloromethane solutions of **1**, **2**, and **3**, the Soret band of each complex became to sharp and intense. The final spectra were almost the same as those of monomer analogues of [Ru(tpp)(CO)(py)], [Ru(tB$_4$porph)(CO)(py)], and [Ru(Hex$_4$porph)(CO)(py)] with ca. 18 nm half-widths. The maximum of the Soret band of the monomer formed in each 3-pyridyl system appeared at the midpoint of the broad Soret bands of the constituent interacting porphyrin subunits as shown in Fig. 3a. ^{1}H NMR measurements at room temperature, where no rotation of pyridyl groups occurred, was used to monitor the progress of the dissociation reaction, that is, the addition of d_5-pyridine (concentration ratio: 250 times) to the $CDCl_3$ solution of **3**, followed by standing for 24 h to complete the dissociation reaction, caused low-field shifts in all of the pyridyl proton signals upon dissociation and concomitantly gave two new sets of signals with the same intensity (9.28 and 9.45 ppm for the protons at the 2nd position, 2-Py), due to constituent porphyrin isomers. This NMR result from the reaction process concretely

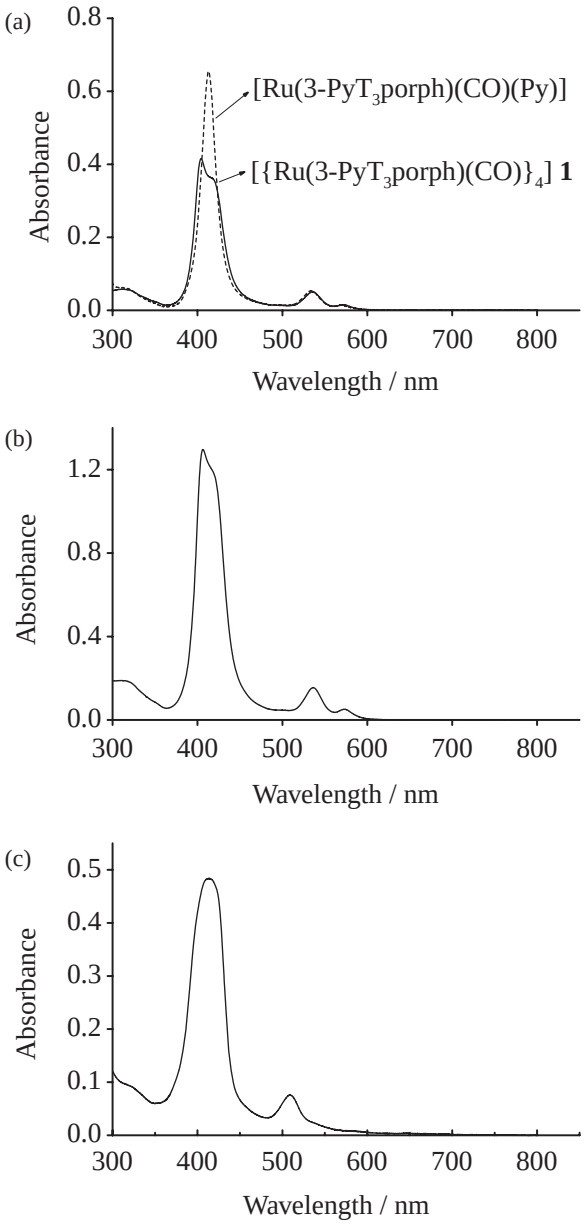

Fig. 3. (a) UV–vis spectral change of **1** by the addition of excess pyridine to the CH_2Cl_2 solution at 23 °C. (b) and (c) are UV–vis spectra of **2** and **4**, respectively, in CH_2Cl_2 at 23 °C. The UV–vis spectrum of **3** is similar to (b).

demonstrates that the tetramers are made from two geometrical isomers of pyridylporphyrin subunits, *cis*- and *trans*-isomers, as illustrated in Fig. 4. The two signals of the 2-Py proton coalesce at around 90 °C to give a single signal by the rotation of the pyridyl groups.

Electrochemical Studies. CVs of the rhombic tetramers and their simulation curves are shown in Figs. 5 and 6, and the redox potentials ($E^{0\prime}$) are listed in Table 2 together with the redox potential differences ($\Delta E^{0\prime}$) in each oxidation step. All of the tetramers underwent two-stage electrochemical oxidations, each of which involved 4-electrons in a manner similar to the square tetramers constructed from 5-(4-pyridyl)porphyrinatoruthenium(II) subunits.[19] By reference to the redox behavior of carbonyl-coordinated porphyrinatoruthenium(II)

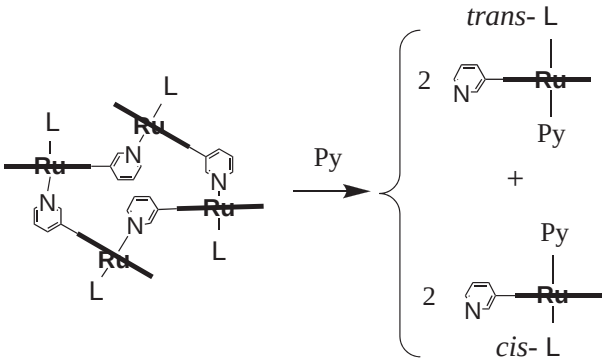

Fig. 4. Dissociation reaction of **3** in d_5-pyridine–$CDCl_3$ at 23 °C.

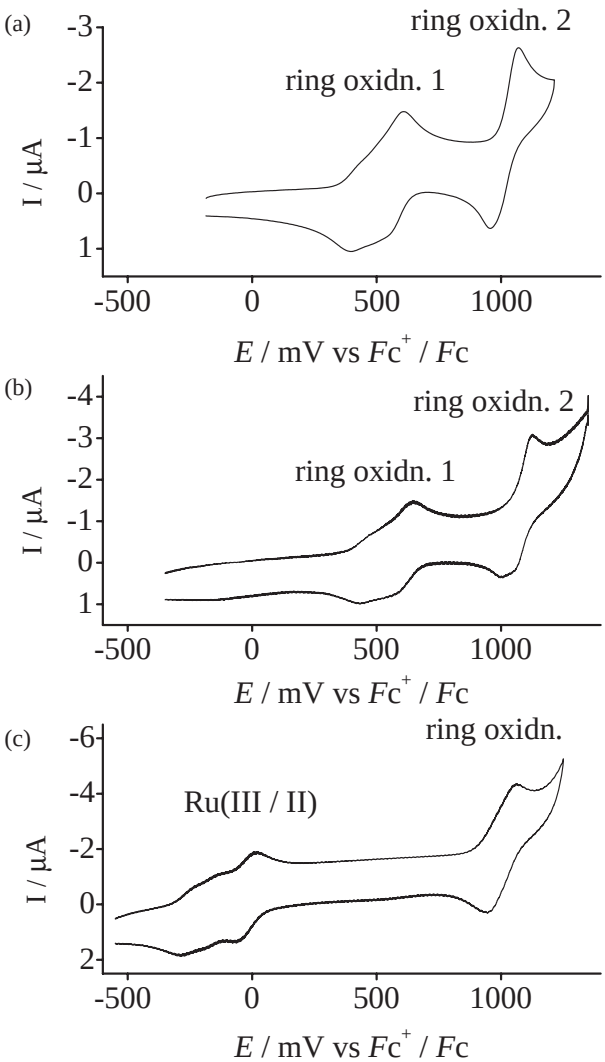

Fig. 5. CVs of tetramers with a rhombic shape in 0.1 M Bu_4NPF_6–CH_2Cl_2 solution at 23 °C. (a) **1**, (b) **2**, and (c) **4**.

analogues,[28] the two oxidation stages in **1**, **2**, and **3** were ascribed to the first and second oxidation processes of their porphyrin rings. The difference in potentials between the first stages and the second stages of the carbonyl-coordinated tetramers was about 400 mV. The difference is almost the same

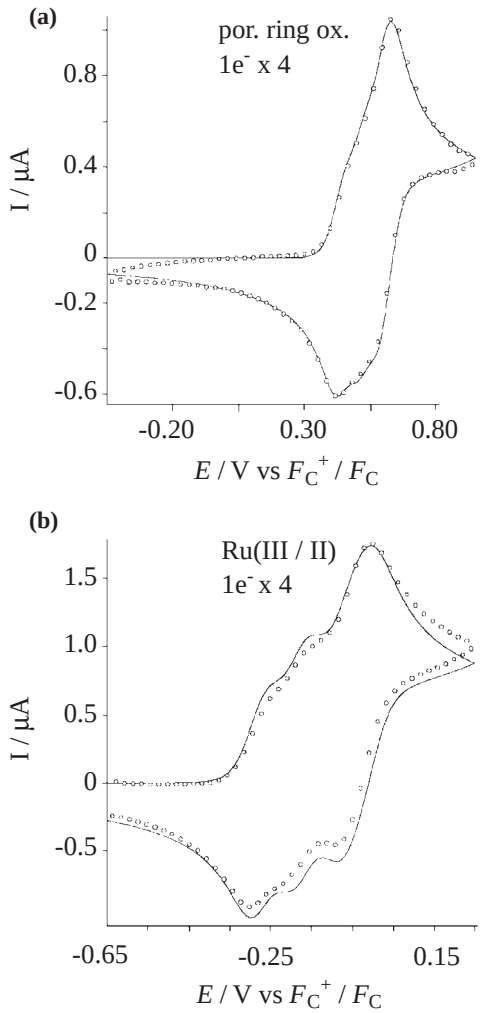

Fig. 6. Simulations of the CVs of (a) **2** and (b) **4**. The solid lines and the dotted lines are simulation curves and experimental curves respectively.

with that of the [Ru(tpp)(CO)] monomer system.[29] In **4**, the first and second stages were ascribed to the oxidation of four ruthenium centers from the oxidation state of II to III and the porphyrin rings, respectively.[19,30] In the carbonyl-coordinated complexes, relative broad waves were observed in the first oxidation stage. Simulations demonstrated that the first stages consisted of stepwise four-one-electron oxidations, as listed in Table 2. The oxidation behavior signifies the presence of electronic interactions among the porphyrinatoruthenium subunits. There were no essential differences among **1**, **2**, and **3** in both $\Delta E^{0\prime}$ and $\Delta E^{0\prime}{}_{\text{total}}$ in their first oxidation stages. The first and second $\Delta E^{0\prime}$ values of ca. 80 and 70 mV were larger than the third $\Delta E^{0\prime}$ values (17–44 mV). $\Delta E^{0\prime}{}_{\text{total}}$ of these tetramers were 177–195 mV. The $\Delta E^{0\prime}{}_{\text{total}}$ values were significantly larger by 47–65 mV than those of square cyclic tetramers, [{Ru(4-PyP$_3$porph)(CO)}$_4$] and [{Ru(4-PyT$_3$porph)(CO)}$_4$].[19] The large electronic interactions must result from less perpendicular arrangements and more flexibilities between porphyrin subunits in the present systems than in the 5-(4-pyridyl)porphyrin square complex systems. This feature is consistent with the broadening of UV–vis spectra as described above. Broad

Table 2. Redox Potentials ($E^{0\prime}$) and $\Delta E^{0\prime}$ Values of 3-Pyridylporphyrinatoruthenium Tetramers[a)]

Complex	$E^{0\prime}$Ru/mV[b)] ($\Delta E^{0\prime}$/mV) $Ru^{III/II}$	$E^{0\prime}{}_1$/mV[b)] ($\Delta E^{0\prime}$/mV) por oxidn. 1	$\Delta E^{0\prime}{}_{\text{total}}$/mV for the 1st step	$E^{0\prime}{}_2$/mV por oxidn. 2
1		378 463 (85) 529 (66) 573 (44)	195	1016
2		382 465 (83) 534 (69) 573 (39)	191	1021
3		366 449 (83) 526 (77) 543 (17)	177	976
4	−275 −171 (104) −64 (107) −15 (49)	986	260	
[Ru(tpp)(CO)][c)]		370		770

a) Redox potentials were corrected with respect to E (Fc^+/Fc) = 0.000 V. b) The potentials were confirmed by CV simulation. c) From Ref. 30, in 0.1 M $Bu_4N(ClO_4)$–CH_2Cl_2.

waves were also observed in the first oxidation stage of **4**. Simulation of the cyclic voltammogram exhibited that the first stage of **4** consisted of stepwise four one-electron oxidations and the largest $\Delta E^{0\prime}{}_{\text{total}}$ value (260 mV). However, broadening of the second oxidation stages for all the rhombic cyclic tetramers was too small to estimate the redox potential of the four one-electron steps, that is, it seems to be pseudo one-step four-electron transfers similar to the square cyclic tetramer systems. This is a common feature in both the rhombic and square cyclic tetramer series. This behavior may reflect the difference in charge densities caused by oxidations in each stage, that is, the charges of the tetramers change largely from zero to plus four in the first oxidation stage but from plus four to plus eight in the second stage.

Conclusion

Self-assembled 5-(3-pyridyl)porphyrinatoruthenium oligomers were synthesized and characterized. The structures were determined to be cyclic tetramers with a rhombic shape by ^{1}H NMR, ESI-MS, and analytical procedures. UV–vis studies exhibited strong excitonic interactions between porphyrin subunits. Electrochemical measurements of all these rhombic tetramers showed a stepwise four-one-electron oxidation in the first porphyrin ring oxidation of **1**–**3** and the Ru oxidation of **4**. As a whole, interactions observed in UV–vis and electrochemical studies between each porphyrinatoruthenium subunit were significantly larger than those of square cyclic tetramers.

We acknowledge funds from a Grant-in-Aid for Scientific Research from the Ministry of Education, Culture, Sports, Science and Technology, Japan (Nos. 08454206 and 17655021).

Supporting Information

H–H COSY NMR spectra of **2** and **4**. UV–vis spectrum and simulated cyclic-voltammograms of **3**. These materials are available free of charge on the web at http://www.csj.jp/journals/bcsj/.

References

1 a) M. A. Thompson, M. C. Zerner, J. Fajer, *J. Phys. Chem.* **1991**, *95*, 5693. b) E. J. P. Lathrop, R. A. Friesner, *J. Phys. Chem.* **1994**, *98*, 3056. c) D. Gust, T. A. Moore, A. L. Moore, S.-J. Lee, E. Bittersmann, D. K. Luttrull, A. Rehms, J. M. DeGraziano, X. C. Ma, F. Gao, R. E. Belford, T. T. Trier, *Science* **1990**, *248*, 199. d) J. P. Collman, J. E. Huchison, M. A. Lopez, R. Guilard, *J. Am. Chem. Soc.* **1992**, *114*, 8066. e) J. P. Collman, J. E. Hutchison, M. S. Ennis, M. A. Lopez, R. Guilard, *J. Am. Chem. Soc.* **1992**, *114*, 8074. f) Y. L. Mest, M. L'Her, *J. Chem. Soc., Chem. Commun.* **1995**, 1441. g) R. Guilard, S. Brandes, C. Tardieux, A. Tabard, M. L'Her, C. Miry, P. Gouerec, Y. Knop, J. P. Collman, *J. Am. Chem. Soc.* **1995**, *117*, 11721. h) X. Peng, N. Aratani, A. Takagi, T. Matsumoto, T. Kawai, I.-W. Hwang, T. K. Ahn, D. Kim, A. Osuka, *J. Am. Chem. Soc.* **2004**, *126*, 4468. i) N. Aratani, A. Osuka, H. S. Cho, D. Kim, *J. Photochem. Photobiol.* **2002**, *3*, 25. j) M.-S. Choi, T. Yamazaki, I. Yamazaki, T. Aida, *Angew. Chem., Int. Ed.* **2004**, *43*, 150. k) Y. Kuramochi, A. Satake, Y. Kobuke, *J. Am. Chem. Soc.* **2004**, *126*, 8668. l) A. Harriman, F. Odobel, J.-P. Sauvage, *J. Am. Chem. Soc.* **1995**, *117*, 9461. m) A. Harriman, J.-P. Sauvage, *Chem. Soc. Rev.* **1996**, *25*, 41.

2 a) L. F. Lindoy, *Nature* **1994**, *368*, 96. b) R. P. Bonar-Law, L. G. Mackay, C. J. Walter, V. Marvaud, J. K. Sanders, *Pure Appl. Chem.* **1994**, *66*, 803. c) A. Osuka, H. Shimidzu, *Angew. Chem., Int. Ed. Engl.* **1997**, *36*, 135. d) M. L. Merlau, M. P. Mejia, S. T. Nguen, J. T. Hupp, *Angew. Chem., Int. Ed.* **2001**, *40*, 4239.

3 a) S. Anderson, H. L. Anderson, J. K. M. Sanders, *Acc. Chem. Res.* **1993**, *26*, 469. b) D. W. J. McCallien, J. K. M. Sanders, *J. Am. Chem. Soc.* **1995**, *117*, 6611.

4 J. Wojaczyński, L. Latos-Grażyński, M. M. Olmstead, A. L. Balch, *Inorg. Chem.* **1997**, *36*, 4548.

5 a) Y. Kobuke, H. Miyaji, *J. Am. Chem. Soc.* **1994**, *116*, 4111. b) Y. Kobuke, H. Miyaji, *Bull. Chem. Soc. Jpn.* **1996**, *69*, 3563.

6 E. B. Fleischer, A. M. Shachter, *Inorg. Chem.* **1991**, *30*, 3763.

7 a) C. A. Hunter, J. K. M. Sanders, *J. Am. Chem. Soc.* **1990**, *112*, 5525. b) Y. H. Kim, D. H. Jeong, D. Kim, S. C. Jeoung, H. S. Cho, S. K. Kim, N. Aratani, A. Osuka, *J. Am. Chem. Soc.* **2001**, *123*, 76. c) Y. Nakamura, I.-W. Hwang, N. Aratani, T. K. Ahn, D. M. Ko, A. Takagi, T. Kawai, T. Matsumoto, D. Kim, A. Osuka, *J. Am. Chem. Soc.* **2005**, *127*, 236. d) I.-W. Hwang, T. Kamada, T. K. Ahn, D. M. Ko, T. Nakamura, A. Tsuda, A. Osuka, D. Kim, *J. Am. Chem. Soc.* **2004**, *126*, 16187. e) J. T. Fletcher, M. J. Therien, *Inorg. Chem.* **2002**, *41*, 331.

8 a) H. M. Goff, E. T. Shimomura, Y. J. Lee, W. R. Scheidt, *Inorg. Chem.* **1984**, *23*, 315. b) G. M. Godziela, D. Tilotta, H. M. Goff, *Inorg. Chem.* **1986**, *25*, 2142. c) A. L. Balch, L. Latos-Grazynski, B. C. Noll, M. M. Olmstead, E. P. Zovinka, *Inorg. Chem.* **1992**, *31*, 2248. d) A. L. Balch, B. C. Noll, M. M. Olmstead, S. M. Reid, *J. Chem. Soc., Chem. Commun.* **1993**, 1088. e) E. Alessio, M. Macchi, S. Heath, L. G. Marzilli, *J. Chem. Soc., Chem. Commun.* **1996**, 1411. f) E. Alessio, S. Geremia, S. Mestroni, I. Srnova, M. Slouf, T. Gianferrara, A. Prodi, *Inorg. Chem.* **1999**, *38*, 2527. g) N. Kariya, T. Imamura, Y. Sasaki, *Inorg. Chem.* **1997**, *36*, 833. h) C. M. Drain, J.-M. Rehn, *J. Chem. Soc., Chem. Commun.* **1994**, 2313. i) H. Yuan, L. Thomas, K. Woo, *Inorg. Chem.* **1996**, *35*, 2808. j) P. J. Stang, J. Fan, B. Olenyuk, *Chem. Commun.* **1997**, 1453.

9 J.-C. Chambron, V. Heitz, J.-P. Sauvage, *The Porphyrin Handbook*, ed. by K. M. Kadish, K. M. Smith, R. Guilard, Academic Press, New York, **2000**, Vol. 6, Chap. 40, pp. 1–42.

10 T. Imamura, K. Fukushima, *Coord. Chem. Rev.* **2000**, *198*, 133.

11 J. Wojaczyński, L. Latos-Grażyński, *Coord. Chem. Rev.* **2000**, *204*, 113.

12 A. K. Burrell, D. L. Officer, P. G. Plieger, D. C. W. Reid, *Chem. Rev.* **2001**, *101*, 2751.

13 R. T. Stibrany, J. Vasudevan, S. Knapp, J. A. Potenza, T. Emge, H. J. Schugar, *J. Am. Chem. Soc.* **1996**, *118*, 3980.

14 N. N. Gerasimchuk, A. A. Mokhir, K. R. Rodgers, *Inorg. Chem.* **1998**, *37*, 5641.

15 K. Funatsu, T. Imamura, A. Ichimura, Y. Sasaki, *Inorg. Chem.* **1998**, *37*, 4986.

16 T. Imamura, K. Funatsu, S. Ye, Y. Morioka, K. Uosaki, Y. Sasaki, *J. Am. Chem. Soc.* **2000**, *122*, 9032.

17 K. Fukushima, K. Funatsu, A. Ichimura, Y. Sasaki, M. Suzuki, T. Fujihara, K. Tsuge, T. Imamura, *Inorg. Chem.* **2003**, *42*, 3187.

18 A. Tsuda, T. Nakamura, S. Sakamoto, K. Yamaguchi, A. Osuka, *Angew. Chem., Int. Ed.* **2002**, *41*, 2817.

19 K. Funatsu, T. Imamura, A. Ichimura, Y. Sasaki, *Inorg. Chem.* **1998**, *37*, 1798.

20 M. Vinodu, Z. Stein, I. Goldberg, *Inorg. Chem.* **2004**, *43*, 7582.

21 A. Tsuda, S. Sakamoto, K. Yamaguchi, T. Aida, *J. Am. Chem. Soc.* **2003**, *125*, 15722.

22 T. S. Balaban, R. Goddard, M. Linke-Schaetzel, J.-M. Lehn, *J. Am. Chem. Soc.* **2003**, *125*, 4233.

23 a) X. Chi, A. J. Guerin, R. A. Haycock, C. A. Hunter, L. D. Sarson, *J. Chem. Soc., Chem. Commun.* **1995**, 2563. b) X. Chi, A. J. Guerin, R. A. Haycock, C. A. Hunter, L. D. Sarson, *J. Chem. Soc., Chem. Commun.* **1995**, 2567.

24 Abbreviations: 3-PyT$_3$porph = 5-(3-pyridyl)-10,15,20-tri-*p*-tolylporphyrinato dianion, 3-PytB$_3$porph = 5-(3-pyridyl)-10,15,20-tris(*p*-*t*-butylphenyl)porphyrinato dianion, 3-PyHex$_3$porph = 5-(3-pyridyl)-10,15,20-tris(*p*-hexyloxyphenyl)porphyrinato dianion, Hex$_4$porph = 5,10,15,20-tetrakis(*p*-hexyloxyphenyl)porphyrinato dianion, 4-PyP$_3$porph = 5-(4-pyridyl)-10,15,20-triphenylporphyrinato dianion, 4-PyT$_3$porph = 5-(4-pyridyl)-10,15,20-tri-*p*-tolylporphyrinato dianion, tB$_4$porph = 5,10,15,20-tetrakis(*p*-*t*-butylphenyl)porphyrinato dianion, tpp = 5,10,15,20-tetraphenylporphyrinato dianion. DDQ = 2,3-dichloro-5,6-dicyano-1,4-benzoquinone, py = pyridine.

25 a) S. S. Eaton, G. R. Eaton, *J. Am. Chem. Soc.* **1977**, *99*, 6594. b) S. S. Eaton, G. R. Eaton, *J. Am. Chem. Soc.* **1975**, *97*, 3660.

26 a) M. Kasha, H. L. Rawls, M. A. El-Bayoumi, *Pure Appl. Chem.* **1965**, *11*, 371. b) M. Kasha, *Radiat. Res.* **1963**, *20*, 55.

27 a) T. Nagata, A. Osuka, K. Maruyama, *J. Am. Chem. Soc.* **1990**, *112*, 3054. b) A. Osuka, B. L. Liu, K. Maruyama, *Chem. Lett.* **1993**, 949.

28 D. P. Rillema, J. K. Nagle, L. F. Barringer, Jr., T. J. Meyer, *J. Am. Chem. Soc.* **1981**, *103*, 56.

29 K. M. Kadish, D. Chang, *Inorg. Chem.* **1982**, *21*, 3614.

30 G. M. Brown, F. R. Hopf, J. A. Ferguson, T. J. Meyer, D. G. Whitten, *J. Am. Chem. Soc.* **1973**, *95*, 5939.